ORIGINAL ARTICLE

Radio-to-TeV γ-ray emission from PSR B1259–63

Andrii Neronov · Maria Chernyakova

Abstract We discuss the implications of the recent X-ray and TeV γ-ray observations of the PSR B1259–63 system (a young rotation powered pulsar orbiting a Be star) for the theoretical models of interaction of pulsar and stellar winds. We show that previously considered models have problems to account for the observed behaviour of the system. We develop a model in which the broad band emission from the binary system is produced in result of collisions of GeV–TeV energy protons accelerated by the pulsar wind and interacting with the stellar disk. In this model the high energy γ-rays are produced in the decays of secondary neutral pions, while radio and X-ray emission are synchrotron and inverse Compton emission produced by low-energy (≤ 100 MeV) electrons from the decays of secondary charged $\pi^{\pm}$ mesons. This model can explain not only the observed energy spectra, but also the correlations between TeV, X-ray and radio emission components.

Keywords Pulsars: individual: PSR B1259–63 · X-rays: binaries · X-rays: individual: PSR B1259–63

PACS 97.60.Gb · 97.80.Jp · 97.10.Me

1 Introduction

PSR B1259–63 is a ~48 ms radio pulsar in a highly eccentric ($e \sim 0.87$), 3.4 year orbit with a Be star SS 2883 (Johnston et al. 1992). The pulsar crosses the Be star disc twice per orbit, just prior to and just after periastron. Unpulsed

A. Neronov (✉) · M. Chernyakova
ISDC, Ch. d'Ecogia 16, 1290 Versoix, Switzerland
e-mail: andrii.neronov@obs.unige.ch

radio, X-ray and γ-ray emission observed from the binary system are produced due to the collision of pulsar wind with the wind of Be star. Observations of the temporal and spectral evolution of the non-thermal emission from the system provide a unique opportunity to probe the physics of the pulsar winds (PW) which is, in spite of the wealth of observational phenomena, and a 40 year old observation history, remains a matter of debate.

The interaction of the PW with the wind from the companion star, is responsible for the formation of a "compactified" pulsar wind nebula (PWN) with the size about the binary separation distance (typically, on AU-scale). Compact size, large matter density and the presence of a strong source (companion star) which illuminates the nebula make the physical properties of the compact PWN significantly different from the ones of their larger scale cousins.

We present the results of the last observation campaign of the PSR B1259–63 system during the 2004 pulsar periastron passage and their applications for the theoretical modelling of the source. We show that most of the observed properties of the system in radio-to-TeV band can be naturally explained within a model of proton-loaded pulsar wind.

2 Multi-wavelength observations of the system during 2004 periastron passage

The upper panel of Fig. 1 shows the X-ray lightcurve of the system (Chernyakova et al. 2006) together with the TeV (Aharonian et al. 2005) and radio (Johnston et al. 2005) lightcurves. For comparison we show also the data from archival X-ray (Kaspi et al. 1995; Hirayama et al. 1999) and radio (Johnston et al. 1999; Connors et al. 2002) observations. Rapid growth of the X-ray flux found in *XMM-Newton* observations of 2004 is correlated with the rapid growth of
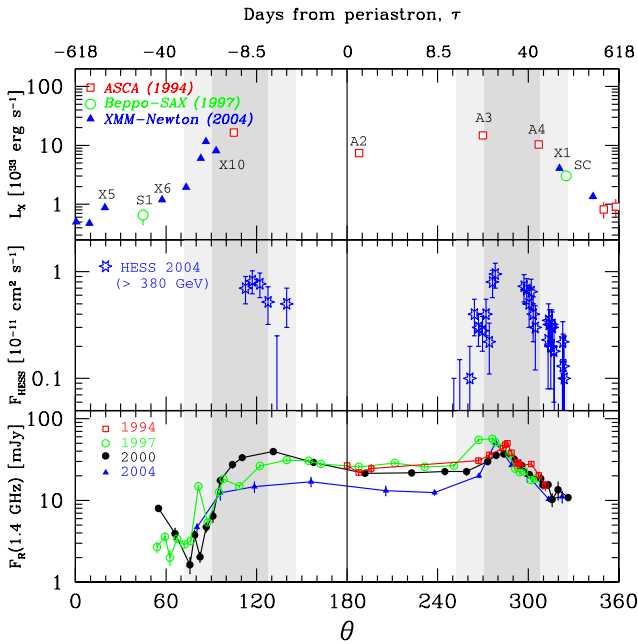
Fig. 1 Comparison between the X-ray (*top*), TeV (*middle*) and radio (*bottom*) lightcurves. *XMM-Newton* observations are marked with *triangles*, *Beppo*SAX ones with *circles*, and *ASCA* ones with *squares*. Data for four different periastron passages. are shown with different colors: *red* (1994), *green* (1997), *black* (2000) and *blue* (2004). *Bottom X axis* shows the orbital phase, θ, *top X axis* shows days from periastron, τ

the unpulsed radio emission from the system. The growth of radio and X-ray flux at these phases can be attributed to the pulsar entering the Be star disk.

Unfortunately, TeV observations start somewhat later and it is not possible to see whether the TeV flux grows during the pre-periastron disk crossing. However, simple geometrical argument tells that the orbital phase θ at which the pulsar should enter the disk for the second time should be shifted by 180° relative to the first entrance. From Fig. 1 one can infer that the first pre-periastron entrance falls roughly between the phases $70° < \theta < 110°$. Thus, the pulsar has to enter the disk again between the phases $250° < \theta < 290°$. Surprisingly, one can clearly see from the middle panel of Fig. 1 that the TeV flux grows in this phase interval. To test the conjecture that the TeV flux grows during the second entrance to the disk we superimpose the pre-periastron X-ray and TeV lightcurves over the post-periastron lightcurves by shifting the phase of the post-periastron data points by −180°. The result is shown in Fig. 2. One can see that in such representation the rise and decrease of both X-ray and TeV flux from the system can be well fitted with a gaussian curve $F(\theta) \sim \exp(-(\theta - \theta_0)^2/(2\Delta\theta_0^2))$. We find that the best fit is achieved with the parameter choice $\theta_0 \simeq 109.1°$, $\Delta\theta_0 \simeq 18.5°$ (the coordinate $\Delta\theta$ along the X-axis of Fig. 2 is, in fact, $\Delta\theta = \theta - \theta_0$). The position of the Gaussian with the above parameters is shown schematically in Fig. 1 by
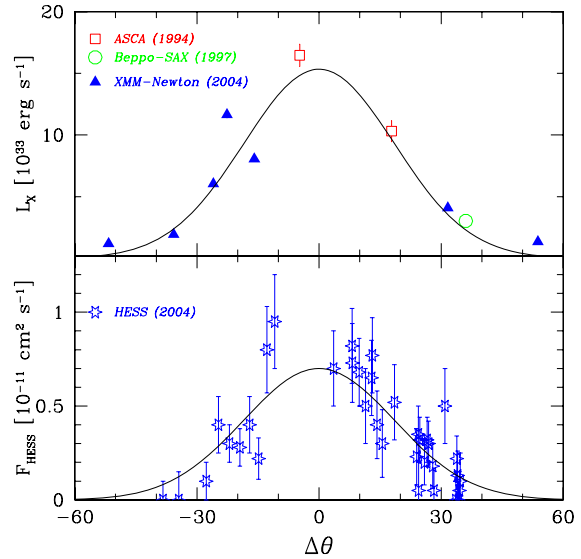

Fig. 2 The X-ray (*top*) and TeV (*bottom*) flux as a function of the relative phase $\Delta\theta = \theta - \theta_0$ (see text for the definition of θ_0). The curves show a fit with a gaussian of the half-width $\Delta\theta_0 = 18.5°$
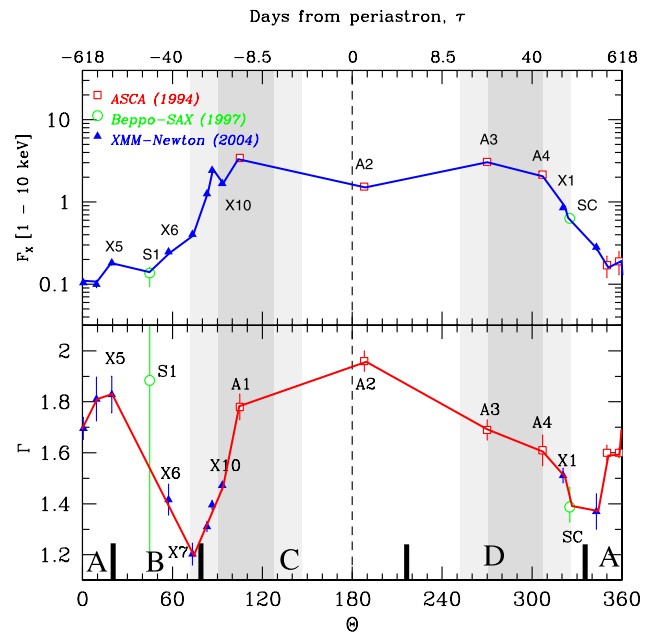

Fig. 3 Evolution of the X-ray photon index Γ_{ph} over the orbital phase θ. Radio flux and spectral index evolution from the 1997 periastron passage (Johnston et al. 1999) are shown in *black*

a shaded area. Denser and lighter shadings in Fig. 1 correspond to the one and two widths of the Gaussian. Depending on the physical mechanisms of the X-ray and TeV emission, the inferred width of the Gaussian $\Delta\theta_0$ gives either an estimate of the "thickness" of the Be star disk, or of the characteristic cooling time of the high-energy particles injected at the phase of the disk passage (see Sect. 5).

The graphical representation of the evolution of the X-ray photon index (the spectrum is well fit by an absorbed powerlaw model) along the orbit is given in Fig. 3. The most remarkable feature of the spectral evolution of the system is the hardening of the X-ray spectrum close to the moment when pulsar enters the Be star disk at the phase $\theta \simeq \theta_0 - 2\Delta\theta_0 \simeq 70°$. One can see that the decrease of the photon index Γ is simultaneous with the onset of the rapid growth of the X-ray flux. Similar hardening of the spectrum down to the photon index $\Gamma_{ph} \simeq 1$ (or, equivalently, down to the spectral index $\alpha \simeq 0$) at the moment of disk entrance is observed in the radio data shown in Fig. 3 in black (Johnston et al. 1999). To the best of our knowledge, neither the hardening of the X-ray spectrum, nor strong correlation between the radio and X-ray flux and spectral index variations was predicted in any of existing models of X-ray emission from the system (see e.g. Tavani and Arons 1997).

3 Implications for theoretical models

Termination of the pulsar wind in the stellar disk leads to the acceleration of ultrarelativistic electrons and subsequent X-ray and gamma-ray emission. Within a simple geometrical picture (Tavani and Arons 1997), the maximum of X-ray (synchrotron) emission is expected during the phases of the disk passage, while the maximum of TeV γ-ray inverse Compton (IC) emission is expected at the moment of the periastron passage. However, surprisingly, the TeV γ-ray lightcurve (middle panel of Fig. 1) has a local minimum in the periastron. The observed X-ray–TeV and radio–X-ray correlations do not agree with the early theoretical predictions (Tavani and Arons 1997; Kirk et al. 1999). To find the range of possible theoretical models which can explain the data it is useful first to make basic qualitative estimates of different time scales present in the system.

3.1 Characteristic cooling times.

Electrons. One of the main differences between the synchrotron and IC mechanisms of X-ray emission is the difference in the cooling time scales. The cooling time of the TeV electrons which can produce synchrotron emission at the energies $\epsilon_S \sim 1$–10 keV in the magnetic field B is

$$t_S \simeq 6 \times 10^2 [B/0.1\,\text{G}]^{-3/2} [\epsilon_S/10\,\text{keV}]^{-1/2}\,\text{s}. \quad (1)$$

The spectrum of optically thin synchrotron emission from the cooled electron population has the photon index $\Gamma_{ph} \geq 1.5$. Any hardening of the X-ray spectrum down to the values $\Gamma_{ph} < 1.5$ (e.g. due to the increased injection of electrons at higher energies) would be "washed out" by the synchrotron cooling at the 10^2–10^3 s time scale. To the contrary, the typical IC cooling time in X-rays is

$$t_{IC\,(T)} \simeq 6 \times 10^5 [R/10^{13}\,\text{cm}]^2 [\epsilon_{IC}/10\,\text{keV}]^{-1/2}\,\text{s}. \quad (2)$$

(we have assumed that the seed photons for the IC scattering come from the companion star of luminosity $L_* \simeq 10^{38}$ erg/s and temperature $T \simeq 2 \times 10^4$ K; the subscript "(T)" indicates that the estimate applies for the Thompson regime). Estimating the size of emission region to be about the binary separation distance, $R \sim 10^{13}$ cm, one can find that electrons emitting IC radiation at 1 keV cool at the day time scales. Observation of the gradual evolution of the X-ray photon index down to $\Gamma_{ph} \simeq 1.2$ and then back to $\Gamma_{ph} \geq 1.5$ on the time scale of several days during the first entrance to the disk (see Fig. 3) is consistent with the IC, rather than synchrotron model of X-ray emission.

In principle, it is possible that X-ray and TeV γ-ray emission from the system are, respectively, low- and high-energy tails of the IC spectrum. Substituting naively the energy of TeV photons $\epsilon_{IC} \sim 1$ TeV into (2) one finds that the time scale of the spectral variability at TeV energies should be very short. However, at TeV energies the IC scattering proceeds in the Klein–Nishina regime and the cooling time in this regime grows with energy,

$$t_{IC\,(KN)} \simeq 8.5 \times 10^3 [\epsilon_{IC}/1\,\text{TeV}]^{0.7} [R/10^{13}\,\text{cm}]^2\,\text{s}. \quad (3)$$

The minimum of the IC cooling time, $\sim 10^3$ s, is reached at roughly at the energy of transition between Thompson and Klein–Nishina regimes, $E_e \sim \epsilon_{IC} \sim 10$–$100$ GeV.

Pulsar wind electrons are able to escape from the region of the dense photon background along the contact surface of pulsar and stellar wind. If the two winds do not mix, the pulsar wind flows along the contact surface with the speed $v_{PW} \sim 10^{10}$ cm/s and escapes beyond the binary separation distance over the time scale

$$t_{esc} \sim R/v_{PW} \simeq 10^3 [R/10^{13}\,\text{cm}]\,\text{s}. \quad (4)$$

This time scale is essentially shorter than the IC cooling time both in X-ray and in the TeV energy bands. Electrons escaping from the innermost region of pulsar wind/stellar wind interaction fill the larger extended region (a "compactified" PWN of the size R_{PWN} of about several binary separation distances) and can loose their energy via IC emission at longer time scales in the less dense photon background produced by the Be star. The escape time from the compact PWN can be naively estimated assuming diffusion in the weak PWN magnetic field. E.g. taking the diffusion coefficient D equal to the Bohm diffusion coefficient at $E_e \sim 1$ TeV and depending on the energy as $D \sim E^{-\alpha}$ ($\alpha = 1$ for the case of Bohm diffusion) one finds

$$t_{PWN} \simeq 10^4 [B/0.1\,\text{G}][E_e/1\,\text{TeV}]^{-\alpha}$$
$$\times [R_{PWN}/10^{13}\,\text{cm}]^2\,\text{s}. \quad (5)$$

During the periods of the pulsar passage through the dense equatorial disk of Be star (typical density of the slow

equatorial stellar wind at the location of the pulsar is $n_{\mathrm{disk}} \sim 10^{10}$–$10^{11}$ cm^{-3}), bremsstrahlung and ionisation energy losses can compete with the IC loss. Indeed, the energy independent bremsstrahlung loss time,

$$t_{brems} = 10^4 [n/10^{11} \text{ cm}^{-3}]^{-1} \text{ s} \qquad (6)$$

is comparable to the IC loss time for the TeV electrons (3) and is shorter than the IC loss time for the X-ray emitting electrons (2). Thus, during the short period of escape from the dense equatorial disk (the escape time is given by (4)) as much as

$$L_\gamma / L_e \simeq t_{esc}/t_{brems} \sim 10\% [n_{\mathrm{disk}}/10^{11} \text{ cm}^{-3}] \qquad (7)$$

of the power in relativistic electrons, L_e, can be converted into the (bremsstrahlung) γ-ray luminosity, L_γ.

Below the electron energy $E_e \sim 350$ MeV the Coulomb energy loss, for which the cooling time scale is given by

$$t_{Coul} \simeq 3 \times 10^3 [n_{\mathrm{disk}}/10^{11} \text{ cm}^{-3}]^{-1} [E_e/100 \text{ MeV}] \text{ s} \qquad (8)$$

dominates over the bremsstrahlung loss. During the periods of the disk passage, essentially 100% of the power output in electrons with energies below the "Coulomb break"

$$E_{Coul} \simeq 30 [n_{\mathrm{disk}}/10^{11} \text{ cm}^{-3}] \text{ MeV} \qquad (9)$$

(estimated from the condition that the Coulomb loss time is equal to the escape time, $t_{Coul} \sim t_{esc}$) will be channeled into the heating of the disk, rather than on emission from the system. As a result, only electrons with energies above E_{Coul} can be injected into the compactified PWN.

3.2 Protons

GeV–TeV energy protons can loose their energy only in interactions with the protons from the stellar wind. The enhancement of the pp interaction rate is expected during the pulsar passage through the dense equatorial disk of Be star. The pp interaction time

$$t_{pp} \simeq 1.6 \times 10^4 [n/10^{11} \text{ cm}^{-3}]^{-1} \text{ s} \qquad (10)$$

is comparable to the electron bremsstrahlung loss time (6). Following the same way of reasoning as in the case of bremsstrahlung, one can find that as much as 10% of the power L_p contained in the PW protons can be channeled in the secondary particles (γ-rays, neutrinos, electrons, positrons) produced in pp interactions. The π^0 decay γ-rays carry away about 1/3 of the power output in pp interactions. Thus, the "γ-ray efficiency" of pp interactions is somewhat lower than the efficiency of bremsstrahlung,

$$L_\gamma / L_p \simeq 0.3 t_{esc}/t_{pp} \sim 3\% [n_{\mathrm{disk}}/10^{11} \text{ cm}^{-3}]. \qquad (11)$$

However, if the PW is proton-dominated, the luminosity of the γ-ray emission from pp interactions can exceed the bremsstrahlung luminosity.

4 IC model of X-ray to TeV emission

Taking into account that the seed photons for the IC scattering have energies of about 10 eV (assuming the temperature of Be star $T \simeq 2 \times 10^4$ K), one can find that the IC emission from electrons of the energy E_e peaks at

$$\epsilon_{IC} \simeq 4 [E_e/10 \text{ MeV}]^2 \text{ keV}. \qquad (12)$$

The energy of the upscattered photons becomes approximately equal to the energy of electrons at

$$\epsilon_{IC, (T \to KN)} \simeq 30 \text{ GeV} \qquad (13)$$

(the transition to the Klein–Nishina regime). If the spectrum of electrons is a simple powerlaw with the spectral index p_e ($dN_e/dE \sim E^{-p_e}$), the IC spectrum below and above the Thompson–Klein–Nishina break is, respectively, $dN_\gamma/dE \sim E^{(p_e+1)/2}$ and $dN_\gamma/dE \sim E^{-p_e+1} \ln E$. The IC emission in the 10–100 GeV energy band is characterized by one more spectral feature. Namely, the IC cooling time of the 10–100 GeV electrons is comparable to the escape time from the compact region with a dense photon background. Estimating the energy of the cooling break in the IC emission spectrum from the condition $t_{esc} \simeq t_{IC, (T)}$ one finds $\epsilon_{IC, \text{cool}} \simeq 4 [R/10^{13} \text{ cm}]$ GeV. Taking into account the coincidence of the cooling break energy with the energy of transition to the Klein–Nishina regime one can not expect to detect the conventional steepening of the IC spectrum above the cooling break because of the reduced efficiency of the IC scattering in the Klein–Nishina regime. One more complication of the detailed calculation of the IC emission spectrum in the GeV–TeV energy band is that in order to explain the observed behaviour of the TeV lightcurve during the periastron passage within the IC model one has to assume that either additional non-radiative cooling mechanism dominates electron energy loss close to the periastron, or a cut-off in the electron spectrum at sub-TeV energies is present (Khangulyan et al. 2006). The combined effect of the above mentioned difficulties makes the detailed predictions for the IC spectrum in the GeV–TeV band quite uncertain and we do not attempt the detailed fit of the observed spectrum in this band. Instead we concentrate on the attempt to fit the general shape of the spectral energy distribution in the X-ray to TeV γ-rayband within the IC model.

Figure 4 shows an example of the fit of the spectrum of PSR B1259–63 in IC model for X-ray to TeV emission. One can see that EGRET upper limit on the flux from the system (Tavani et al. 1996) requires the presence of a break in the IC spectrum at the energies $E \sim 1$ MeV. In the model fit shown in the figure, the electron spectrum below the break at $E_e = 100$ MeV has the spectral index $p_e = 2$, while above the break the spectrum steepens to $p_e + 1 = 3$. It is clear that the overall shape of the IC spectrum in the keV to TeV energy band agrees well with the data.
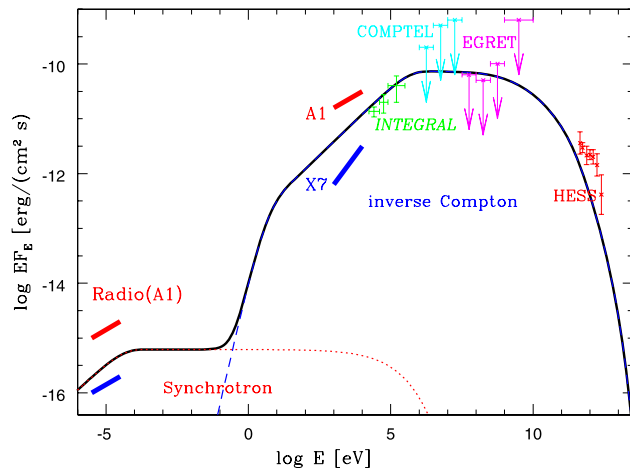
Fig. 4 IC model fit for the X-ray to TeV spectrum of the source. Radio emission is synchrotron from electrons which produce X-ray IC flux

The energy of the break in the electron spectrum ($\sim$100 MeV) is close to the energy of the Coulomb break given by (9). As it was discussed above, electrons with energies below E_{Coul} loose all their energy via the severe Coulomb loss before they are able to escape from the dense equatorial disk of Be star to the less dense PWN. As a result, regardless of the initial injection spectrum of electrons from the PW, the spectrum of electrons injected in the compact PWN has a low-energy cut-off at the energy $\sim E_{Coul}$. The IC cooling of electrons in the PWN leads to the formation of the characteristic powerlaw tail of electron distribution below E_{Coul} with $p_e = 2$. The electron spectrum above the energy E_{Coul} (assumed to be a powerlaw with the spectral index $p_e = 3$ in the model fit of Fig. 4) is determined by the balance of acceleration and energy losses in the pulsar/stellar wind shock region.

Electrons responsible for the X-ray IC emission produce synchrotron radiation in radio band at the characteristic frequency

$$\epsilon_S \simeq 1.5[B/0.1\ \text{G}][E_e/30\ \text{MeV}]^2\ \text{GHz}. \tag{14}$$

The ratio of the synchrotron to IC luminosity is given by the ratio of the energy densities of the magnetic field and radiation,

$$L_S/L_{IC} = 2 \times 10^{-4}[B/0.1\ \text{G}]^2[R_{\text{PWN}}/10^{13}\ \text{cm}]^2. \tag{15}$$

The radio luminosity of the system is some 4 orders of magnitude lower than the X-ray luminosity. This imposes a restriction on the possible strength of magnetic field in the X-ray emission region,

$$B \leq 0.1[R_{\text{PWN}}/10^{13}\ \text{cm}]^{-1}\ \text{G}. \tag{16}$$

In the model fit of Fig. 4 we have chosen the magnetic field strength $B = 0.03$ G and assumed the size of X-ray/radio emission region $R_{\text{PWN}} \sim 3 \times 10^{13}$ cm.

5 Alternative mechanisms of TeV γ-ray emission

5.1 Bremsstrahlung

The IC model for the keV-to-TeV spectrum has a difficulty to explain the observed correlation of the radio, X-ray and TeV emission because the cooling and escape times of electrons emitting IC radiation in X-ray and TeV bands are different. Since the non-pulsed radio emission from the system is most probably related to the passage of the pulsar through the disk of Be star, an explanation of the observed correlation requires a physical mechanism which would explain the increase of the TeV flux during the disk passage. At least two mechanisms of interaction of the pulsar wind with the Be star disk can lead to the increase of TeV emission: bremsstrahlung and proton-proton interactions.

As it is discussed above, the bremsstrahlung cooling time in the dense Be star disk (6) can be comparable to the IC cooling time both for the highest energy electrons above TeV and for electrons with energies below 1 GeV (see (2, 3)). The bremsstrahlung cooling time can be comparable to the escape time from the compact equatorial disk so that up to 10% of the power of the pulsar wind can be emitted in the form of bremsstrahlung radiation. Figure 5 shows the fit for the γ-ray spectrum of the system with a combination of IC and bremsstrahlung emission. The electron spectrum is supposed to be a cut-off powerlaw with the spectral index $p_e = 2.5$ and cut-off energy $E_{cut} = 20$ TeV. Note that the EGRET upper limit imposes a restriction on the spectrum of electrons because the bremsstrahlung spectrum has the photon index $\Gamma_{ph} \simeq p_e$. Assuming that the electron spectrum continues to lower energies without a break would violate the EGRET bound on the flux. A break at the energy $E \simeq 350$ MeV was assumed in the electron spectrum in the model fit of Fig. 5. The break at this particular energy is naturally expected in the bremsstrahlung scenario, because below this energy the ionization loss dominates over the bremsstrahlung loss, which leads to the hardening of the electron spectrum by $\Delta p_e \simeq 1$ at low energies.

5.2 pp interactions

If the pulsar wind is proton-loaded, interactions of the pulsar wind protons with the protons from the dense Be star disk provide an additional source the TeV γ-ray emission. As it is discussed above, the "γ-ray efficiency" of pp interactions is a factor of several lower than that of bremsstrahlung, but the relative contributions of bremsstrahlung and pp interactions into the γ-ray emission depend on the proton-to-electron ratio of the PW. If the pulsar wind is mostly proton loaded, the π^0 decay emission can dominate over the γ-ray emission from the pulsar wind electrons. An example of the fit to the TeV γ-ray spectrum within the pp model is
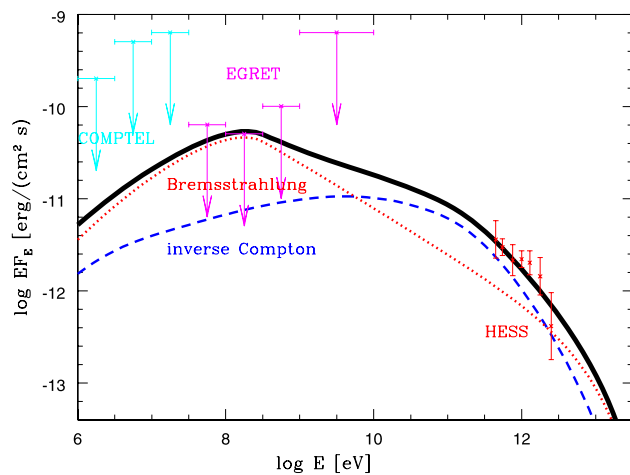
Fig. 5 Comparison of bremsstrahlung and IC contributions to the γ-ray flux. See text for the values of parameters used for the model fits
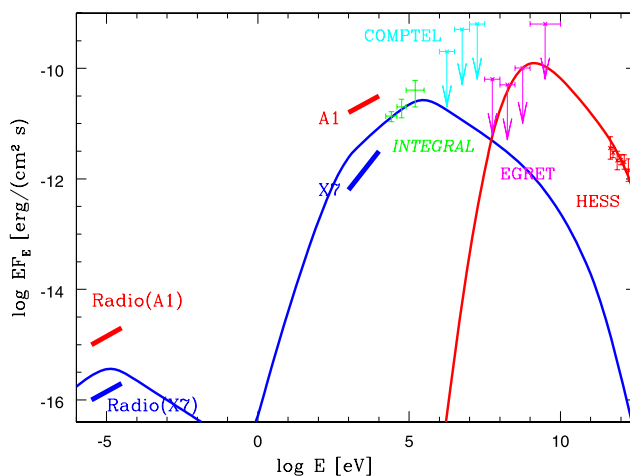

Fig. 6 Broad band spectrum in the pp model. γ-ray emission is produced via neutral pion decays (*red line*) while radio and X-ray emission are, respectively, synchrotron and IC radiation from electrons/positrons produced in the charged pion decays

shown in Fig. 6. We have assumed a powerlaw spectrum of protons with the spectral index $p_p = 2.6$ for the model fit. Similarly to the case of bremsstrahlung, the EGRET upper limit on the flux imposes a restriction on the spectrum of the protons at several GeV energies. However, contrary to the bremsstrahlung case, the spectrum of π^0 decays γ-ray emission has a low energy cut off below GeV energy and the restriction on the spectrum of the protons is rather weak. In fact, in the model fit of Fig. 6 the proton spectrum is described by a single powerlaw from GeV to TeV energies. It is important to note that in this case the luminosity of the source in the 10 GeV energy band is higher than in the TeV band.

Bremsstrahlung or pion decay emission dominate the TeV flux, the TeV luminosity is just proportional to the density of the Be star disk at the location of the pulsar. This means that in this case the parameters of the Gaussian that approximately fits the TeV lightcurve (Fig. 2) should be identified with the equatorial plane position (θ_0) and width ($\Delta\theta_0$) of the disk. Within such interpretation the disk appears to be geometrically thick and the calculation of the phases of disappearance/reappearance of the pulsed emission has to be done by calculating the column density of the disk along the line of sight for different positions of the pulsar. Fixing the phases of disappearance/reappearance of the pulsed emission to the known values, one can obtain a constraint on the radial density profile of the disk and/or inclination of the disk w.r.t. the line of sight. However, if inverse Compton emission gives a contribution comparable to the pion decay or bremsstrahlung, the derivation of the disk parameters from the shape of the TeV lightcurve is not possible.

The most important feature of the model with pp interactions is that it can explain the broad band spectrum of the system from radio to TeV energy band. The idea is that the synchrotron and IC emission from the secondary electrons produced in the decays on charged pions is emitted in the radio and X-ray bands, respectively, while the bremsstrahlung emission from the secondary electrons, emitted in the γ-ray band gives a sub-dominant contribution, compared to the π^0 decay emission. Figure 6 shows an example of the fit to the broad band spectrum of the system within the pp interactions model. Since the emission in radio, X-ray and TeV bands is produced via one and the same process (pp interactions), the observed correlation of the radio, X-ray and TeV flux is naturally explained. Besides, the observed hardening of the X-ray spectrum during a several-day period following the moment of the entrance of the pulsar to the disk of Be star is explained by the low energy cut-off at $\sim$100 MeV in the spectrum of secondary electrons. Such a cut off arises (a) because of the kinematics of the pion decays and (b) because of the efficient Coulomb cooling of electrons with energies below 100 MeV during the escape from the Be star disk.

The pp interaction scenario is attractive because of one more reason: in this model the overall energy balance of the system is evident. Indeed, in the "purely electronic" models it is not clear why the system is "radiatively inefficient": the spin-down luminosity of the pulsar is $\simeq 10^{36}$ erg/s, but the bolometric luminosity is just $L < 10^{34}$ erg/s, which accounts for no more than one percent of the spin-down luminosity. To the contrary, within "protonic" model one has to assume that proton-loaded PW carries a significant fraction of the spin-down power. As it is explained above, in the pp model the efficiency of conversion of the power contained in the protons into

the γ-ray emission is several percents, (see (11)) which explains the γ-ray luminosity $L_\gamma \sim 10^{34}$ erg/s.

The *pp* model can be readily tested with the future observations of the system in the 10 GeV energy band with GLAST. Indeed, from Fig. 6 one can see that in the *pp* model the EGRET upper limit on the flux at 10 GeV should be close to the actual level of the γ-ray flux from the system. This means that the detection of the system during the periastron passage with a more sensitive instrument, like GLAST should not be a problem.

References

Aharonian, F., et al.: Astron. Astrophys. **442**, 1 (2005)

Chernyakova, M., Neronov, A., Lutovinov, A., Rodriguez, J., Johnston, S.: Mon. Not. Roy. Astron. Soc. **367**, 1201 (2006)

Connors, T.W., Johnston, S., Manchester, R.N., McConnell, D.: Mon. Not. Roy. Astron. Soc. **336**, 1201 (2002)

Hirayama, M., Cominsky, L.R., Kaspi, V.M., Nagase, F., Tavani, M., Kawai, N., Grove, J.E.: Astrophys. J. **521**, 718 (1999)

Johnston, S., Manchester, R.N., Lyne, A., Bailes, M., Kaspi, V.M., Qiao, G., D'Amico, N.: Astrophys. J. **387**, L37 (1992)

Johnston, S., Manchester, R.N., McConnell, D., Campbell-Wilson, D.: Mon. Not. Roy. Astron. Soc. **302**, 277 (1999)

Johnston, S., Ball, L., Wang, N., Manchester, R.N.: Mon. Not. Roy. Astron. Soc. **358**, 1069 (2005)

Kaspi, V.M., Tavani, M., Nagase, F., Hirayama, M., Hoshino, M., Aoki, T., Kawai, N., Arons, J.: Astrophys. J. **453**, 424 (1995)

Khangulyan, D., Hnatic, S., Aharonian, F., Bogovalov, S.: astro-ph/0605663 (2006)

Kirk, J.G., Ball, L., Skjaeraasen, O.: Astropart. Phys. **10**, 31 (1999)

Tavani, M., Arons, J.: Astrophys. J. **477**, 439 (1997)

Tavani, M., et al.: Astron. Astrophys. Supp. **120**, 221 (1996)